Supplementary Information (SI) for Nanoscale.

This SI replaces the original version published on 13 Mar 2025

Supplementary material

Programming a multiplex lanthanide nanoparticle for customized cancer treatment with real time efficiency feedback

Hongxia Zhao[a,d], Wei Chen[b], Yu Zhu[a], Zhicong Chao[a], Jiahui Sun[a], Qing Zhang[a], Hongqian Guo[b], Huangxian Ju[a], and Ying Liu[a,c]*

[a]State Key Laboratory of Analytical Chemistry for Life Science, School of Chemistry and Chemical Engineering, Nanjing University, Nanjing 210023, China

[b]Department of Urology, Affiliated Drum Tower Hospital, Medical School of Nanjing University, Institute of Urology, Nanjing University, Nanjing 210023, China

[c]Chemistry and Biomedicine Innovation Center, Nanjing University, Nanjing 210023, China

[d]College of Pharmacy and Chemistry & Chemical Engineering, Taizhou University, Jiangsu, Taizhou 225300, China

* Corresponding author. E-mail: yingliu@nju.edu.cn

1. Experimental Procedures

1.1 Materials. Rare-earth(III) anhydrous chloride (Yb, Gd, Nd, Ce, Er) were purchased from Alfa Asea and used as received. Sodium hydroxide (NaOH), ammonium fluoride (NH_4F), cyclohexene, 1-octadecene (ODE), oleic acid (OA), ethanol, chloroform, dimethyl sulfoxide (DMSO), dimethyl formamide (DMF), 1,3-diphenylisobenzofuran (DPBF), rose bengal (RB), 4-(2-hydroxyerhyl)piperazine-1-erhanesulfonic acid (HEPEs), 3-[(3-cholamidopropyl)dimethylammonio]-1-propanesulfonate (CHAPs), ethylene diamine tetraacetic Acid (EDTA), dithiolthreitol (DTT), 4-aminophenylmercuric acetate (APMA), tris(hydroxymethyl)aminomethane (Tris), β-mercaptoethanol (β-ME), matrix metalloproteinase 2 (MMP 2), matrix metalloproteinase 9 (MMP 9), alkaline phosphatase (ALP) from bovine intestinal mucosa were purchased from Sigma-Aldrich (Saint Louis, MO, USA). Sodium chloride (NaCl), calcium chloride ($CaCl_2$), magnesium chloride ($MgCl_2$), ferrous chloride ($FeCl_2$), zinc chloride ($ZnCl_2$), trichloromethane ($CHCl_3$), methanol (MeOH), ethyl acetate, petroleum ether were supplied by Sinopharm Chemical Reagent Co., Ltd. (Shanghai, China). 1,2-distearoyl-sn-glycero-3-phosphoethanolamine-N-[methoxy(polyethylene glycol)] (DSPE-PEG, MW=2000), dibenzocyclooctyl and cRGD functionalized DSPE-PEG (DSPE-PEG-DBCO, MW=2000, DSPE-PEG-cRGD, MW=5000) were purchased from Tanshtech. Cyanine7.5 maleimide(Cy7.5-Mal) was purchased from Lumiprobe. Recombinant human Cleaved Caspase-3 protein (Caspase-3) was purchased from Abcam (Shanghai, China). Recombinant human furin protein (Furin) was purchased from Abcam (Shanghai, China). Caspase-3 substrate peptide K(N_3)ADVEDAC (Mw=876.15) was synthesized and purified by Sangon Biotech Co., Ltd (Shanghai, China) with purity greater than 98.0%. Dulbecco's modified Eagle's medium (DMEM), 2′,7′-dichlorofluorescein diacetate (DCFH-DA), 6-diamidino-2-phenylindole (DAPI), medium3-(4,5-dimethylthiazol-2-yl)-2-diphenyltetrazolium (MTT), annexin V-FITC apoptosis detection kit and HCCLM3 cells were purchased from Keygen Biotech (Nanjing, China). Fetal bovine serum (FBS) was purchased from (Thermo Fisher Scientific, USA). Mouse IgG(Immunoglobulin G), mice interferon-γ (IFN-γ), and tumor necrosis factor-α (TNF-α)

ELISA kits, PE Anti-Mouse CD3 Antibody, FITC Anti-Mouse CD4 Antibody and APC Anti-Mouse CD8a Antibody were purchased from Elabscience Biotechnology Co.,Ltd. (Wuhan, China). All chemicals were analytical grade and used without further purification.

1.2 Characterizations. Transmission electron microscopic (TEM) images were acquired on JEM-2100 transmission electron microscope (JEOL Ltd., Japan). Powder X-ray diffraction (XRD) analysis was performed on ARL X'TRA XRD system (Thermo Fisher Scientific, USA). Dynamic light scattering (DLS) analysis was performed on ZetaPlus 90 Plus/BI-MAS (Brook haven, USA). High-performance liquid chromatography (HPLC) was carried out on Thermo Scientific Dionex Ultimate 3000 with CH_3CN/H_2O (1%CF_3COOH) as the eluents. Ultraviolet-visible-near-infrared light (UV-Vis-NIR) absorption spectra were recorded with UV-3600 UV-vis-NIR spectrophotometer (Shimadzu Company, Japan). The cell images were captured on TCS SP8 STED 3X confocal laser scanning microscope (CLSM) (Leica, Germany). MTT assays were conducted on Hitachi/Roche System Cobas 6000 (Bio-Rad, USA). Flow cytometric analysis was performed with CytoFLEX Flow Cytometer (Beckman-Coulter, USA). Upconversion luminescence (UCL) spectra and NIR-IIb fluorescence spectra were detected by a FL spectrometer F980 (Edinburgh Instruments, UK) under external adjustable 808 nm laser and 980 nm laser. *In vivo* NIR-II fluorescence imaging was carried out by using NIR-II *In Vivo* Imaging System (Series III 900/1700, Suzhou NIR-Optics Technologies Co., Ltd., China) equipped with 808 nm and 980 nm diode lasers and 1500 nm long-pass (LP 1500) filter. A thermoelectric cooled 640 × 512-pixel 2D InGaAs focal plane array microscopic camera (detecting range: 900–1,700 nm, Princeton Instruments, USA) was used to carry out high-magnification molecular imaging. 1,100 nm long-pass filter (Thorlabs) was used for 980 nm excitation light and 1,500 nm long-pass filter (Thorlabs) was used for 808 nm excitation light for imaging taken.

1.3 Synthesis of luminescence core $NaGdF_4$:Yb,Er,Ce for lanthanide nanoparticles (LNPs). The synthesis of luminescence core $NaGdF_4$:Yb,Er,Ce was referred to our previous work[1]. $GdCl_3$ (0.2 mmol), $YbCl_3$ (0.73 mmol), $CeCl_3$ (0.05 mmol) and $ErCl_3$ (0.02 mmol) were mixed with 9 mL OA and 15 mL ODE, and stirred at 150 °C for 90 min under

vacuum. After the solution was cooled down to 45 °C, 10 mL methanol solution containing 4 mmol NH_4F and 2.5 mmol NaOH was added dropwise and stirred at 45 °C for 30 min. Subsequently, the solution was kept at 110 °C for 15 min to remove methanol, heated to 300 °C and kept for 80 min under nitrogen.

After cooling down to room temperature, the as-obtained $NaGdF_4$:Yb,Er,Ce was centrifuged, washed twice with acetone and ethanol respectively, and finally dispersed in 10 mL of cyclohexane for further use.

1.4 Preparation of inert shell $NaGdF_4$ precursor and NIR absorption shell $NaYbF_4$:Nd precursor for LNPs. $GdCl_3$ (1.2 mmol) was mixed with 4 mL of OA and 12 mL of ODE, heated to 150 °C for 90 min in vacuum. The reaction solution was then cooled down to 45 °C. A solution of NaOH (3 mmol) and NH_4F (4.8 mmol) in methanol (12 mL) was added and the resultant mixture was stirred for half an hour. The reaction mixture was heated to 110 °C for 15 min to completely remove methanol and obtain inert shell $NaGdF_4$ precursor.

NIR absorption shell $NaYbF_4$:Nd precursor was prepared according to the above procedure by replacing $GdCl_3$ with $YbCl_3$/$NdCl_3$ (molar ratio of 1:1).

1.5 Synthesis of $NaGdF_4$:Yb,Er,Ce@$NaYbF_4$:Nd@$NaGdF_4$ LNPs. Core-multi shell structured LNPs $NaGdF_4$:Yb,Er,Ce@$NaYbF_4$:Nd@$NaGdF_4$ was prepared with one-pot successive layer-by-layer (SLBL) protocol[2]. 5 mL of the above-obtained upconversion core $NaGdF_4$:Yb,Er,Ce was mixed with 4 mL of OA and 12 mL of ODE. Cyclohexane was removed by keeping the solution at 85 °C for 30 min. The reaction mixture was then switched to N_2 flow and further heated to 300 °C. Subsequently, 4 mL of the above prepared NIR absorption shell precursor $NaYbF_4$:Nd (1 mmol) was injected into the reaction mixture and kept at 300 °C for 30 min for the shell growth. The above shell coating step was repeated 2 times to get a satisfactory thickness for absorption shell. The as-obtained $NaGdF_4$:Yb,Er,Ce@$NaYbF_4$:Nd was precipitated, washed with acetone and ethanol, and re-dispersed in cyclohexane for future use.

The above-obtained $NaGdF_4$:Yb,Er,Ce@$NaYbF_4$:Nd was mixed with 3.0 mL of OA and 9.0 mL of ODE, kept at 85 °C for 30 min, and heated to 300 °C in N_2 flow. 4 mL of the above prepared inert shell precursor $NaGdF_4$ (1.2 mmol) was injected into the reaction mixture and kept at 300 °C for 30 min. The above shell coating step was repeated 2 times to get a satisfactory thickness for inert shell. The as-obtained LNPs $NaGdF_4$:Yb,Er,Ce@$NaYbF_4$:Nd@$NaGdF_4$ was precipitated with acetone, washed twice with acetone and ethanol, and re-dispersed in cyclohexane for future use.

1.6 Absolute quantum yield measurement. The absolute quantum yield was evaluated following a literature reported protocol with slight modifications[3]. Fluorescence spectrometer (F980, Edinburgh Instruments) was incorporated with an integrating sphere to collect the excitation and emission light through multiple reflections over the entire surface of the sphere. LNPs emissions in the visible and NIR-II regions were produced by a 980/808 nm laser (3 W/cm^2). The scatter measurements were conducted with a neutral density filter (optical density = 3, ~0.09% transmittance at 808 nm, ~0.15% transmittance at 980 nm, Guangzhou Hengyang Optical Technology Co., Ltd) placed between the integrating sphere and the monochromator/detector. The filter was then removed for the emission measurements. The integrated area for scatter/absorption was multiplied by 1000 to correct for filter attenuation. The quantum yields of LNPs were calculated using the following equation:

$$QY = \frac{\text{photons emitted}}{\text{photons absorbed}} = \frac{\text{E[sample]} - E[blank]}{\text{S[blank]} - \text{S[sample]}}$$

Where sample is LNPs disperses in cyclohexane, blank is cyclohexane. QY is the quantum yield. E[sample] and E[blank] are the emission intensities of LNPs and blank solution respectively. S[blank] and S[sample] are the scatter intensities of excitation light for LNPs solution and blank solution, respectively.

1.7 Preparation of azide and Cy7.5 functionalized caspase-3 substrate peptide (N_3-Pep-Cy7.5). Cy7.5-Mal was dissolved in DMF (2.5 mM, 180 μL), mixed with caspase-3 substrate K(N_3)ADVEDAC peptide (10 mM, HEPEs buffer,

pH 7.4, 300 μL) and stirred overnight at room temperature in dark. The crude product was purified by HPLC and freeze-dried to get N_3-Pep-Cy7.5 with a yield of 91%.

1.8 Preparation of RB/N_3-Pep-Cy7.5 functionalized LNPs (LNPs-RB/Pep) and RB/N_3-Pep-Cy7.5/cRGD functionalized LNPs (LNPs-RB/Pep/cRGD). To disperse LNPs in aqueous solution, 10 mg of the above-obtained cyclohexane dispersed LNPs and 20 mg of DSPE-PEG/DSPE-PEG-DBCO (mass ratio = 1:1) were dispersed in chloroform, mixed in a 10 mL flask, and stirred overnight. Chloroform solvent was then slowly evaporated under nitrogen atmosphere. The residue was dispersed in 10 mL ultrapure water, and ultra-sonicated at 80 °C for 5 min. The as-obtained PEG-DBCO functionalized LNPs (LNPs-PEG-DBCO) were centrifuged, washed with ultrapure water three times, and dispersed into HEPES buffer (10 mM, pH 7.4) for future use.

200 μL of above obtained LNPs-PEG-DBCO (5 mg/mL) was mixed with varying volumes of N_3-Pep-Cy7.5 (1 mM, HEPEs buffer, pH 7.4), kept shaking for 4 h in dark to conjugate N_3-Pep-Cy7.5 (1.6 mM, 0, 5, 10, 20, 40, 60, 80 μL) to LNPs-PEG-DBCO via click reaction. After centrifuged at 14000 rpm for 20 min to remove the unreacted N_3-Pep-Cy7.5, the as-obtained LNPs-Pep was wash for 3 times, and diluted to 0.5 mL for future use.

100 μL of RB dispersed DMSO (2 mM) was mixed with 1 mg of above-obtained LNPs-Pep in 1 mL ultrapure water, and stirred overnight in dark. The as-obtained LNPs-RB/Pep was centrifuged, washed with ultrapure water, and re-dispersed in ultrapure water for future use.

To endow the as-obtained LNPs-RB/Pep with tumor cell targeting capability, RB, N_3-Pep-Cy7.5, and cRGD functionalized LNPs was prepared according to the same procedure as described above by replacing DSPE-PEG/DSPE-PEG-DBCO (mass ratio = 1:1) mixture with DSPE-PEG/DSPE-PEG-DBCO/DSPE-PEG-cRGD (mass ratio of 9:10:1) mixture.

1.9 *In vitro* response of LNPs-RB/Pep to caspase-3. 500 μL of the above obtained LNPs-RB/Pep (2 mg/mL) was incubated with various concentrations of caspase-3 protease (0, 1, 2, 3, 4, 5, 6, 8, 10 U/mL) at 37 °C for 3 h. The mixture solution was then centrifuged (14000 rpm, 10 min), and re-dispersed in 500 μL ultrapure water. NIR-IIb fluorescence spectra of the above samples (2 mg/mL) were recorded under 808 nm and 980 nm excitations.

To verify response selectivity, 500 μL of LNPs-RB/Pep (2 mg/mL) was reacted with nonspecific protease including caspase-1 (1 μg/mL, 5 μL), ALP (1 μg/mL, 5 μL), Furin (10 ng/mL, 10 μL), Gram B (0.5 μg/mL,10 μL), MMP-2 (1 μg/mL, 5 μL), MMP-9 (1 μg/mL, 5 μL), and other interfering substance including 100 μM K^+, Mg^{2+}, $^1O_2$, •OH and H_2O_2,

respectively. The above mixtures were incubated at 37 °C for 3 h, and NIR-IIb fluorescence spectra were measured according to the same procedure above. MMP-2 and MMP-9 reaction was conducted in 50 mM Tris(hydroxymethyl)aminomethane (Tris) containing 10 mM $CaCl_2$, 150 mM NaCl (pH 7.5) at 37 °C for 1 h (protease was pre-activated with 1 mM 4-aminophenylmercuric acetate (APMA). ALP reaction was conducted in 10 mM Tris containing 2 mM $MgCl_2$, 0.1 mM $ZnCl_2$ (pH 8.0). Gram B reaction was conducted in 50 mM Tris containing 100 mM NaCl, 25 mM $CaCl_2$, 0.1% Tween (pH 7.4). Furin reaction was conducted in 100 mM HEPEs containing 0.5% Triton X-100，1 mM $CaCl_2$，1 mM β-ME (pH 7.5). Hydroxyl radical (•OH) was produced via Fenton reaction by adding ferrous chloride ($FeCl_2$) into10 equiv. of H_2O_2 solution. $^1O_2$ was produced from a mixed reaction of $NaMoO_4$ (10 mM) and H_2O_2 (10 mM).

1.10 Stability of LNPs-RB/Pep/cRGD. To verify structure stability of LNPs-RB/Pep/cRGD, it (2 mg/mL) was dispersed in saline and DMEM containing 10% FBS, and downconversion and upconversion emission spectra were recorded at different time intervals. To verify photostability of LNPs-RB/Pep/cRGD, it (2 mg/mL) was irradiated 10 min by 808 nm and 980 nm (1 W/cm^2) laser, and downconversion and upconversion emission spectra were recorded.

1.11 Cell Culture. HCCLM3 cells were cultured in DMEM cell culture medium complemented with 10% FBS, streptomycin (100 mg/mL) and penicillin (100 mg/mL) at 37 °C in a (95%) humidified atmosphere containing 5% CO_2. Cell numbers were counted by a Petroff-Hausser cell counter (USA).

1.12 Characterization of ROS generation. To characterize $^1O_2$ generation *in vitro*, 1 mL of LNPs-RB/Pep dispersed ethanol solution (5 mg/mL) was mixed with 20 μL of DPBF ethanol solution (2.5 mg/mL), and irradiated with 980 nm laser at 0.8 W/cm^2 for 60 min. DPBF absorbances were measured from supernatant at 412 nm every 10 min. Control experiments were also performed with the same procedure in the absence of NIR irradiation and under 808 nm laser and 980 nm (0.05 W/cm^2) irradiation respectively.

DCFH-DA (10 mM) stock solution was diluted by 1000 times with PBS buffer of pH=7 and incubated in dark for 20 min. LNPs-RB/Pep aqueous solution (2 mg/mL, 20 μL) was mixed with 480 μL of above DCFH-DA solution, and irradiated with 980 nm laser at 0.8 W/cm^2 for 30 min. Finally, the fluorescence intensity was measured by fluorescence spectrophotometer with anexcitation wavelength of 488 nm and an emission wavelength of 525 nm, respectively. Control experiments were also performed with the same procedure in the absence of NIR irradiation and under 808 nm laser and 980 nm (0.05 W/cm^2) irradiation respectively.

The intracellular $^1O_2$ generation was characterized by incubating HCCLM3 cells with LNPs-RB/Pep/cRGD (200 μL, 200

μg/mL) for 4 h, the culture medium was then replaced with fresh DMEM containing DCFH-DA (200 μL, 50 μM). After continuously cultured for 30 min, the cells were washed with PBS. The as-treated cells were irradiated for 30 min under 980 nm laser irradiation at 0.8 W/cm^2 and 0.05 W/cm^2, respectively (with 5 min break after each 10 min exposure). CLSM fluorescence images were taken by excitation at 488 nm, and the emission was collected from 500 to 550 nm. Control experiments were performed by incubating HCCLM3 cells with LNPs-RB/Pep/cRGD (200 μL, 200 μg/mL) for 4 h in the absence of NIR irradiation and under 808 nm laser irradiation respectively.

1.13 Cytotoxicity of LNPs-RB/Pep/cRGD. Cytotoxicity of LNPs-RB/Pep/cRGD was evaluated by MTT assay. HCCLM3 cells were cultured in a 96-well plate (1 × 10^4 per well) for 24 h. The cell culture medium was then replaced with fresh DMEM containing serial concentrations of 200 μL LNPs-RB/Pep/cRGD (0, 25, 50, 100, 200 μg/mL) for 4 h and then were irradiated for 30 min under 980 nm laser irradiation at 0.8 W/cm^2, and continuously incubated for 24 h. Subsequently, 20 μL of 0.5 mg/mL MTT solution was added into each well. After additional incubation of 4 h, the medium was carefully aspirated and replaced with 150 μL of DMSO. After briefly shaking for 15 min, the absorbance was measured with Bio-Rad microplate reader at 490 nm. Control experiments were also performed according to the same procedure in the absence of NIR irradiation, only under 980 nm (0.05 W/cm^2) irradiation and only under 808 nm (0.05 W/cm^2) irradiation. The relative cell viability was calculated using the following equation: cell viability rate (%) = $OD_{treatment}$ / $OD_{control}$ × 100%.

To evaluate the therapeutic effect of LNPs-RB/Pep/cRGD, HCCLM3 cells were treated with different concentrations of LNPs-RB/Pep/cRGD for 4 h, washed with PBS two times, and exposed under 980 nm light with a power density of 0.8 W/cm^2 for 30 min (with 5 min break after each 10 min exposure). The above treated cells were then continuously cultured for 24 h to analyze the cell viability with MTT assay. Control experiments were performed by exposing HCCLM3 cells under 808 nm laser or in the absence of NIR irradiation respectively, and MTT assay was performed subsequently to analyze cell viability.

1.14 Cell Apoptosis Assay. HCCLM3 cells (2 × 10^5 per well) were seeded into a 12-well plate and incubated with 200 μL of LNPs-RB/Pep/cRGD (200 μg/mL) in the cell incubator for 4 h, irradiated with 980 nm laser at 0.8 W/cm^2 for 0 min, 10 min, 20 min, 30 min, 40 min (with 5 min break after each 10 min exposure) and continuously incubated for 12 h. The cells were then collected and washed with PBS thrice, stained with the mixture of 5.0 μL Annexin V-FITC and 5.0 μL propidium iodide for 15 min, and measured with flow cytometry to evaluate cell apoptosis.

1.15 *In vitro* caspase-3 imaging via immuno-fluorescence. 200 μL of HCCLM3 cells were seeded in a 4-well confocal

dish with ~5 × 10^4 cells per well, and incubated with 200 μL LNPs-RB/Pep/cRGD (200 μg/mL) in the cell incubator for 4 h, irradiated with 980 nm laser at 0.8 W/cm^2 for 0 min, 10 min, 20 min, 30 min, 40 min (with 5 min break after each 10 min exposure) respectively, and continuously incubated for 4 h. Cells were washed twice with PBS, then fixed in 4% paraformaldehyde solution for 10 min at room temperature. The fixed cells were washed with PBS for another three times, permeabilized with a PBS solution containing 1% Triton X-100 at 4°C for 10 minutes. After rinsed with PBS for another two times, the cells were blocked with a PBS solution containing 5% bovine serum albumin for 10 min at 37°C. The as-treated cells were incubated with caspase 3 primary antibody IgG overnight at 4°C, followed by incubated with Cy3 conjugated anti-IgG antibody for 2 h at 37°C. After three washes with PBS, the stained cells were labeled with DAPI for 10 min, and captured images with a CLSM imaging system. The control group was set by pretreating HCCLM3 cells with free substrate peptide (KADVEDAC, 2 mM) for 2 h. The as-treated cells were subsequently incubated with 200 μL LNPs-RB/Pep/cRGD (200 μg/mL) for 4 h, exposed under 980 nm laser at 0.8 W/cm^2 for 40 min as controls.

1.16 *In vivo* imaging of LNPs-RB/Pep/cRGD. Subcutaneous tumor liver cancer-bearing mice were purchased from Pusheng Biomedical Biotech. Co., Ltd. (Nanjing, China). All *in vivo* experiments were performed in accordance with the NIH guidelines for the care and use of laboratory animals (NIH Publication no. 85-23 Rev. 1985) by qualified operators (Certificate Number of 220195151). All animal procedures were performed in accordance with the Guidelines for Care and Use of Laboratory Animals of Nanjing University and approved by the Animal Ethics Committee of Nanjing University with approval number of IACUC-2303006.

The Balb/c nude mice (4-5 weeks, female) were each subcutaneously injected with 1 × 10^7 HCCLM3 cells in the right leg to generate subcutaneous tumor animal modal. The tumor-bearing mice were used for imaging and in vivo experiments when the tumor volumes reached approximately 60 mm^3. The tumor bearing mice were intravenously injected with 200 μL LNPs-RB/Pep/cRGD suspension (2 mg/mL, saline) and reinjected at 2 h intervals to increase tumor accumulation, and NIR-IIb images at 1550 nm were acquired under 980 nm laser (0.05 W/cm^2) at different time points post injection. 2 L/min oxygen flow with 1.5% isoflurane was used for mice anesthesia during injection and *in vivo* imaging process.

1.17 *In vivo* NIR-IIb fluorescence imaging guided PDT. After administration, the systematic circulation of LNPs-RB/Pep/cRGD probe was traced by measuring its NIR-IIb fluorescence at 1550 nm under 980 nm laser at 0.05 W/cm^2 with a NIR-II *In Vivo* Imaging System with 1500 nm long-pass (LP 1500) filter. Optimal time for LNPs-RB/Pep/cRGD accumulation at tumor position was determined as 9 h post-injection, which was chosen to excute photodynamic

therapy (PDT) with 40 min (with 5 min break after each 10 min exposure) of intense 980 nm (0.8 W/cm^2) irradiation.

The tumor-bearing mice for PDT were randomly divided into five groups (n=3), and respectively administrated with (i) saline, (ii) LNPs-RB/Pep/cRGD (2 mg/mL, 200 μL) in the absence of 980 nm laser irradiation, (iii) LNPs-RB/Pep/cRGD (2 mg/mL, 200 μL) with 10 min of 980 nm laser irradiation, (iv) LNPs-RB/Pep/cRGD (2 mg/mL, 200 μL) injected group with 20 min of 980 nm laser irradiation, and (v) LNPs-RB/Pep/cRGD (2 mg/mL, 200 μL) injected group with 40 min of 980 nm laser irradiation. 980 nm (0.8 W/cm^2) NIR irradiation was performed with 5 min break after each 10 min exposure. The injection and irradiation were repeated every other two days for seven times. The tumor volumes along with the weight of the mice were recorded every 2 days. All the animals were scarificed at day 14. The tumor volumes were calculated as $V = (L \times W^2)/2$, where L and W are the length and width of the tumor, respectively. The tumor and major organs including heart, spleen, kidney, liver, and lung were harvest for the histopathological analysis and immunohistochemistry.

1.18 *In vivo* caspase-3 ratiometric NIR-IIb fluorescence imaging. To *in vivo* evaluate caspase-3 generation, NIR-IIb images at 1550 nm of mice were acquired under 808 nm and 980 nm (0.05 W/cm^2) excitations respectively at different time points after PDT. The ratio analysis of $F_{1550, Ex808}$ / $F_{1550, Ex980}$ was performed to obtain the corresponding ratio imaging. To evaluate the amount of cleaved Cy7.5 peptide fragment in excretions, the mice were placed in the metabolism cages during experiment for urine collection. Cy7.5 fluorescence was measured by NIR-II *in vivo* imaging system under 808 nm excitation with 900 nm long-pass (LP 900) filter after PDT.

1.19 Customized cancer therapy according to real time efficiency feedback. To evaluate contribution of customized treatment to therapeutic efficiency enhancement, the tumor-bearing mice for customized-PDT were randomly divided into two groups (n=3), and both administrated with LNPs-RB/Pep/cRGD (2 mg/mL) and 10 min of 980 nm laser irradiation. According to the *in vivo* ratiometric imaging and urinary fluorescence detection results, group (i) was treated with twice of 10 min 980 nm NIR irradiation then adjusted to 40 min for five times. According to tumor size observation, group (ii) was treated with four times of 10 min 980 nm NIR irradiation then adjusted to 40 min for three times. Injection and irradiation were repeated every two days. 980 nm NIR irradiation was performed with 5 min break after each 10 min exposure. The tumor volumes along with the weight of the mice were recorded every 2 days. All the animals were sacrificed at day 14. The tumor volumes were calculated as $V = (L \times W^2)/2$, where L and W are the length and width of the tumor, respectively.

1.20 *In vivo* excretion of LNPs-RB/Pep/cRGD. Healthy BALB/c nude mice (n=3) were intravenously injected with 200

μL LNPs-RB/Pep/cRGD (2 mg/mL) to study its *in vivo* excretion. The mice were imaged under 980 nm irradiation to monitor the excretion of RB/Pep/cRGD during 0-8 day. Mice feces were collected at predetermined time points during 8 days treatment period. The major organs of mice were collected at day 8, weighted and dissolved in 2 mL nitric acid at 70 °C for 12 h. Each sample was diluted with deionized water and the corresponding Gd^{3+} concentration was determined by ICP-AES.

1.21 ***The immunogenicity of LNPs-RB/Pep/cRGD.*** For the mice immunization study, two groups of BALB/c mice (6 to 8 weeks, female) were intravenously administrated with 200 μL the (2 mg/mL) or saline respectively, and boosted with equal doses of formulations 7 days later. Blood samples were collected on days 7 and 14 after LNPs-RB/Pep/cRGD administration to quantify IgG and cytokines IFN-γ and TNF-α generations using an ELISA kit (Elabscience Biotechnology Co., Ltd. (Wuhan, China)).

To measure *in vivo effector memory T cell immune response,* mice were scarified by cervical dislocation, then splenocytes were aseptically removed. Analysis of mouse T cell population isolation from spleen were assayed as previously literature described[4]. Briefly, approximately 1×10^6 live cells were incubated with LNPs-RB/Pep/cRGD (200 μg/mL) at 37 ^oC for 4h. The cells were then washed with 2% FBS in PBS and stained with 5 μL PE Anti-Mouse CD3 antibody, 5 μL FITC Anti-Mouse CD4 antibody, and 5 μL APC Anti-Mouse CD8 antibody for 20 min in dark at 4 ^oC. Finally, cells were washed with PBS and re-suspended in 2% FBS/PBS. Stained cells were analyzed using using flow cytometry.

2. Supplemental Data

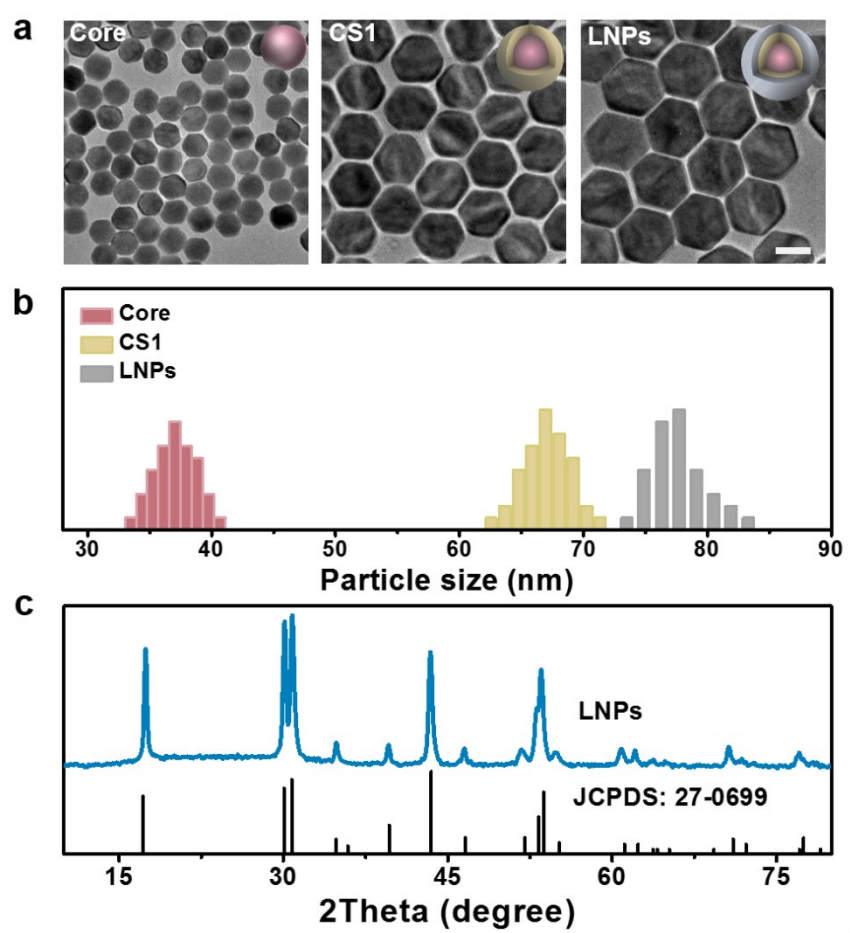

Figure S1. (a) TEM images and (b) size distribution of LNP $NaGdF_4$:Yb,Er,Ce (core), layered structure $NaGdF_4$:Yb,Er,Ce@$NaYbF_4$:Nd (CS1), and $NaGdF_4$:Yb,Er,Ce@$NaYbF_4$:Nd@$NaGdF_4$ (LNPs), Scale bars are 50 nm. (c) XRD patterns of LNPs and *β*-$NaGdF_4$ (JCPDS: 27-0699).

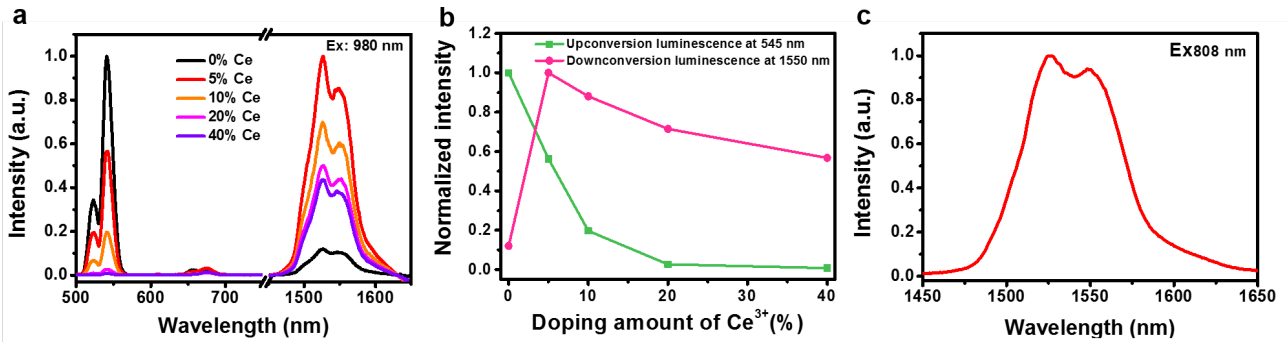

Figure S2. (a) Upconversion and downconversion luminescence spectra of $NaGdF_4$:Yb,Er,Ce (Ce% = 5, 10, 20, 40) under 980 nm excitation and (b) their corresponding normalized luminescence intensity. (c) Downconversion luminance spectrum of LNPs under 808 nm excitation.

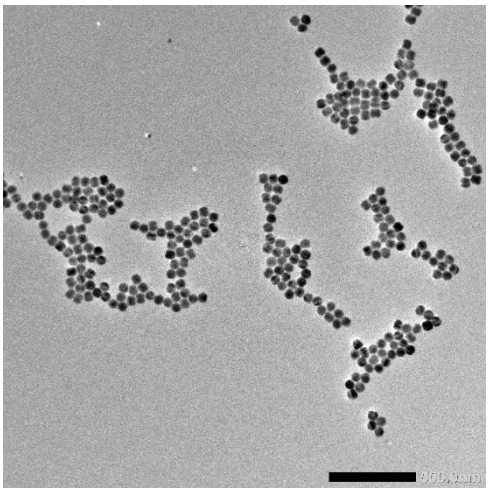

Figure S3. TEM Image of LNPs-PEG-DBCO. Scale bar is 500 nm.

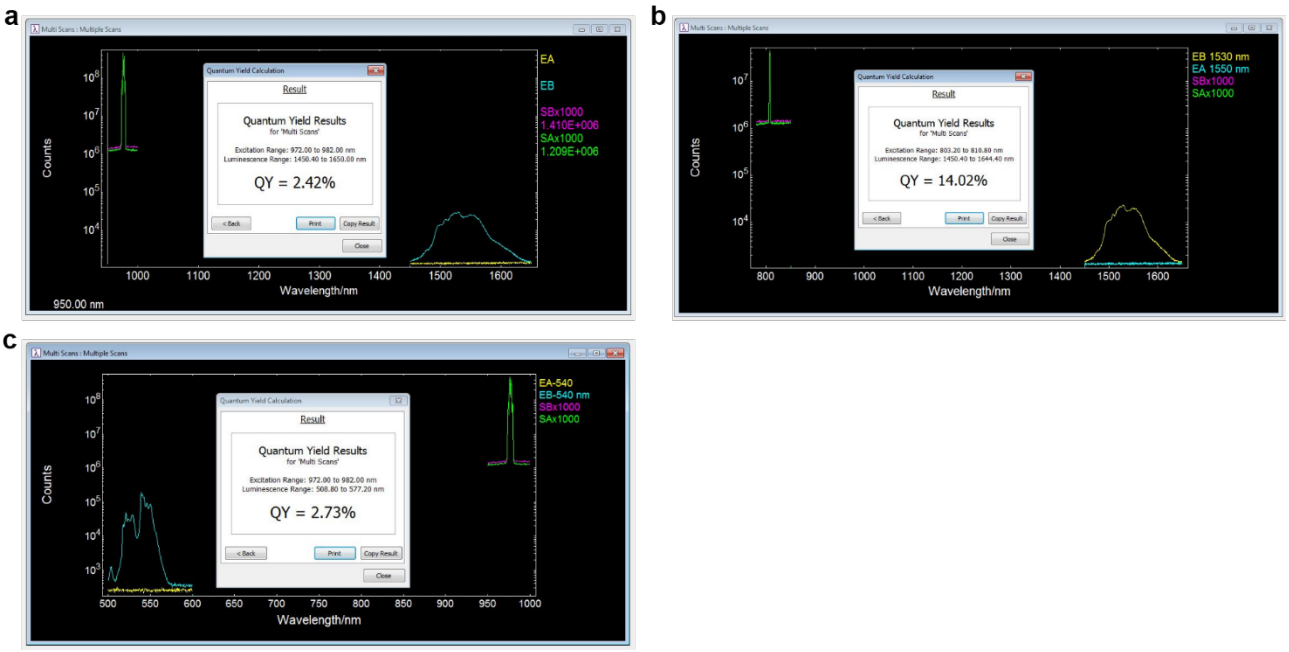

Figure S4. The raw data of absolute quantum yield of LNPs at NIR-IIb emission range (1450-1650 nm) under (a) 980 nm, (b) 808 nm laser excitation (3 W/cm^2), and (c) visible emission range (500-600 nm) under 980 nm laser excitation (3 W/cm^2) in cyclohexane measured by integrating sphere. The integrated area for scatter/absorption was multiplied by 1000 to correct for filter attenuation.

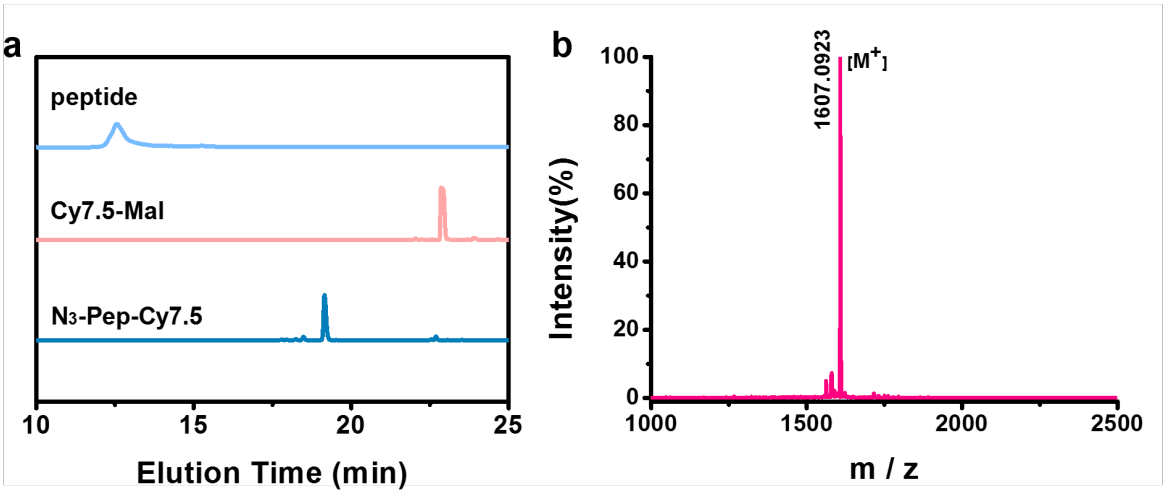

Figure S5. (a) High Performance Liquid Chromatography (HPLC) and (b) MALDI-TOF mass spectrum of N_3-Pep-Cy7.5.

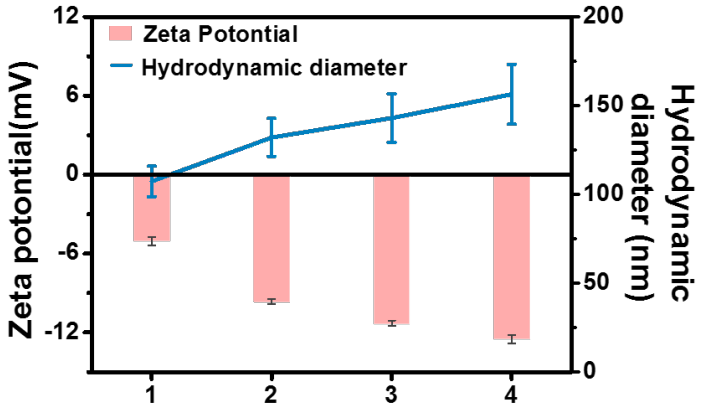

Figure S6. Hydrodynamic diameter and zeta potential of (1) LNPs-PEG-DBCO, (2) LNPs-Pep (3) LNPs-RB/Pep and (4) LNPs-RB/Pep/cRGD. The error bars indicate mean ± S.D. (n = 3).

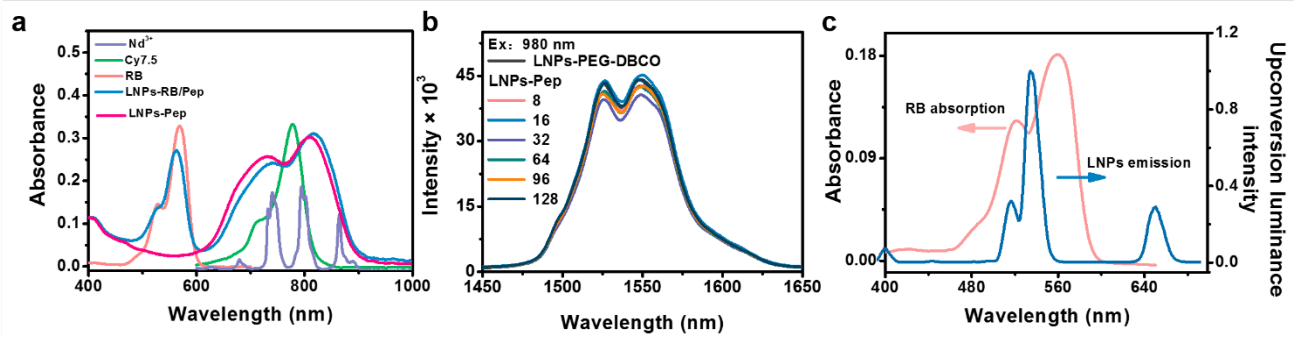

Figure S7. (a) Absorption spectra of Nd^{3+}, Cy7.5, RB, LNPs-Pep and LNPs-RB/Pep. (b) Downconversion emission luminance spectra of LNPs-Pep (N_3-Pep-Cy7.5 loading concentrations from 8 to 128 nmol/mg) under 980 nm (c) Upconversion emission luminance spectrum of LNPs under 980 nm excitation and UV/Vis absorption spectrum of

RB.

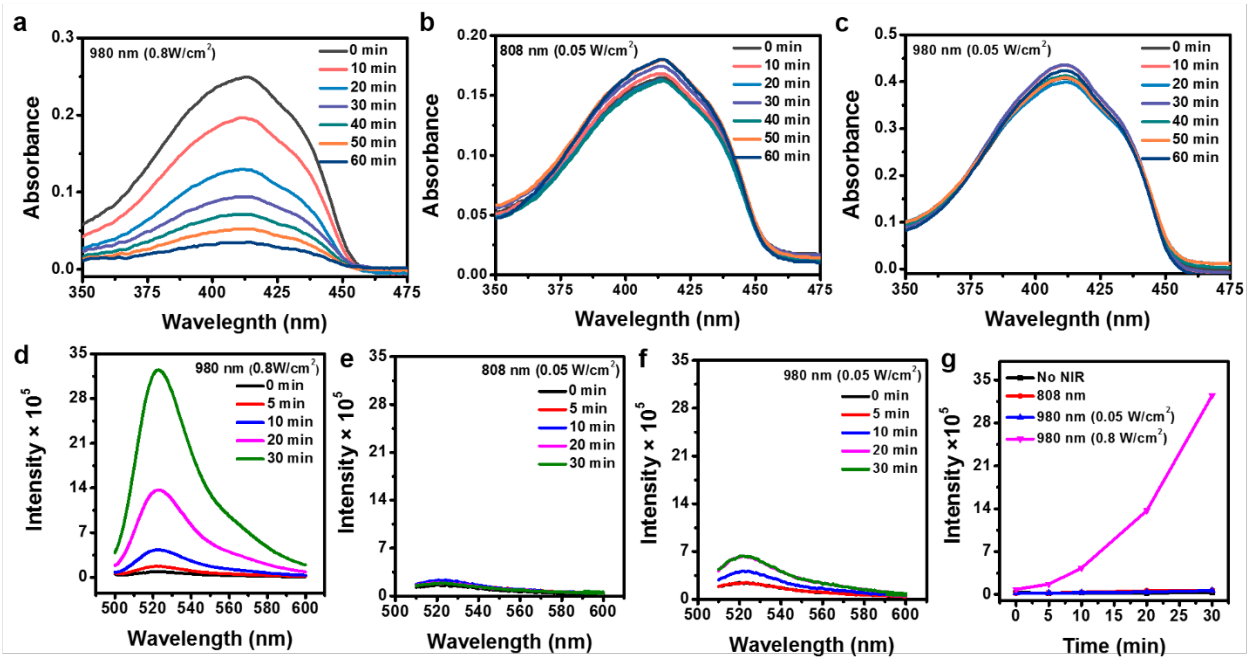

Figure S8. Absorbance spectra of DPBF after incubation with LNPs-RB/Pep (2 mg/mL) under (a) 980 nm, 0.8 W/cm^2, (b) 808 nm, 0.05 W/cm^2 and (c) 980 nm, 0.05 W/cm^2 irradiation for 60 min, respectively. The fluorescence spectra of DCFH-DA solution (pH=7.4) incubation with LNPs-RB/Pep under (d) 980 nm (0.8 W/cm^2), (e) 808 nm (0.05 W/cm^2) and (f) 980 nm (0.05 W/cm^2) irradiation of 30 min. and (g) corresponding time dependent characteristic fluorescence signal of DCFH-DA at 522 nm.

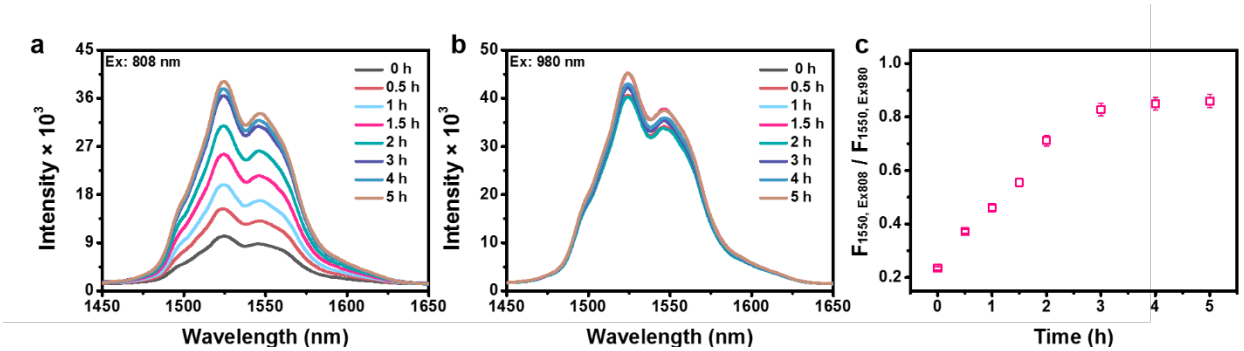

Figure S9. Time dependent NIR-IIb luminance spectra of LNPs-RB/Pep (2 mg/mL, 500 μL) with caspase-3 (8 U/mL) incubation different times (0-5 h) at 37 °C under (a) 808 nm, (b) 980 nm excitation and (c) $F_{1550, Ex808}$ / $F_{1550, Ex980}$ ratio change.

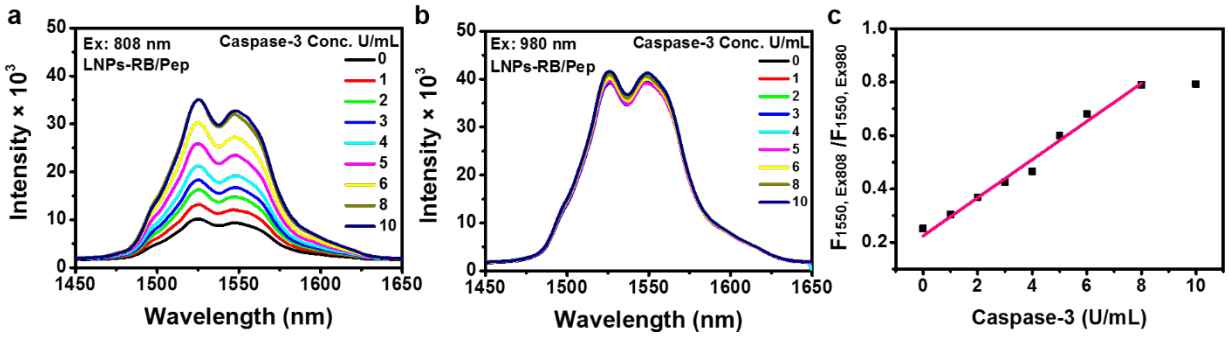

Figure S10. NIR-IIb luminance spectra of LNPs-RB/Pep (2 mg/mL, 500 μL) under (a) 808 nm, (b) 980 nm excitation in response to caspase-3 (0-10 U/mL) at 37 °C for 3h, and (c) linear relationship of $F_{1550,\ Ex808}$ / $F_{1550,\ Ex980}$ corresponding to caspase-3 concentration.

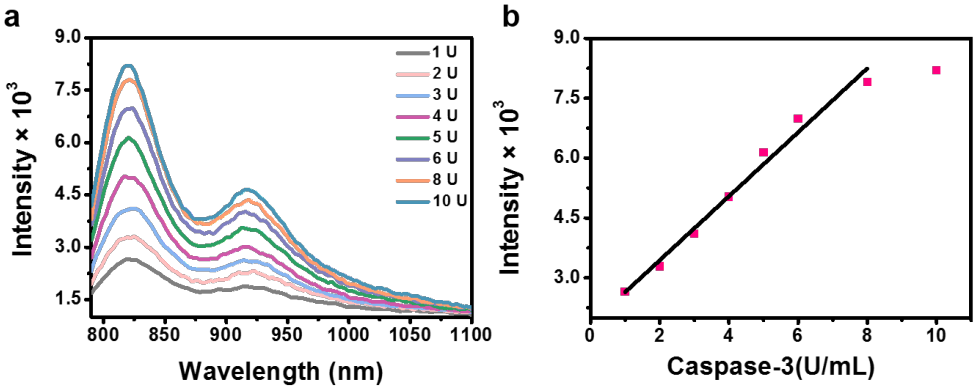

Figure S11. Fluorescence emission spectra of supernatant for LNPs-RB/Pep (2 mg/mL, 500 μL) incubating with different concentrations caspase-3 (1-10 U/mL) at 37 °C for 3h and (b) the linear relationship between emission peak intensity at 820 nm corresponding to caspase-3 concentration.

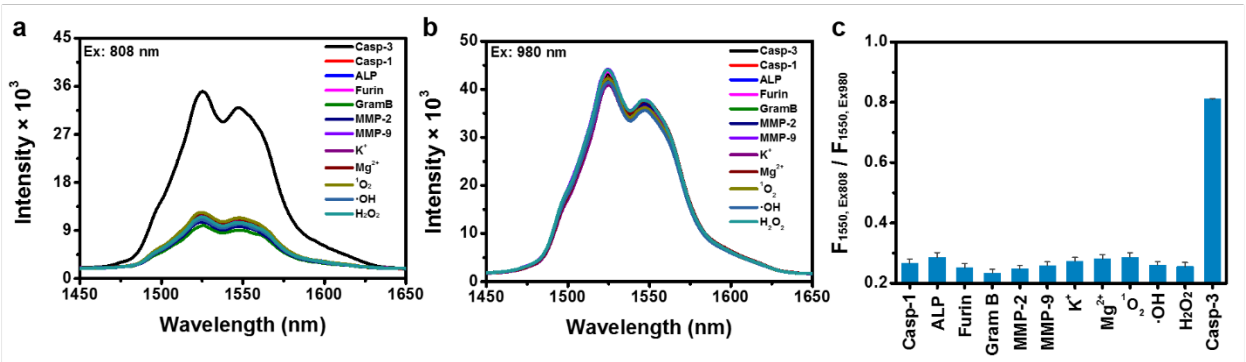

Figure S12. NIR-IIb fluorescence spectra of LNPs-RB/Pep (2 mg/mL, 500 μL) in response to various nonspecific enzymes, biomolecules and ions under (a) 808 nm, (b) 980 nm excitation, respectively, and corresponding (c) $F_{1550,\ Ex808}$ / $F_{1550,\ Ex980}$ ratios. The error bars indicate means ± S.D. (n = 3).

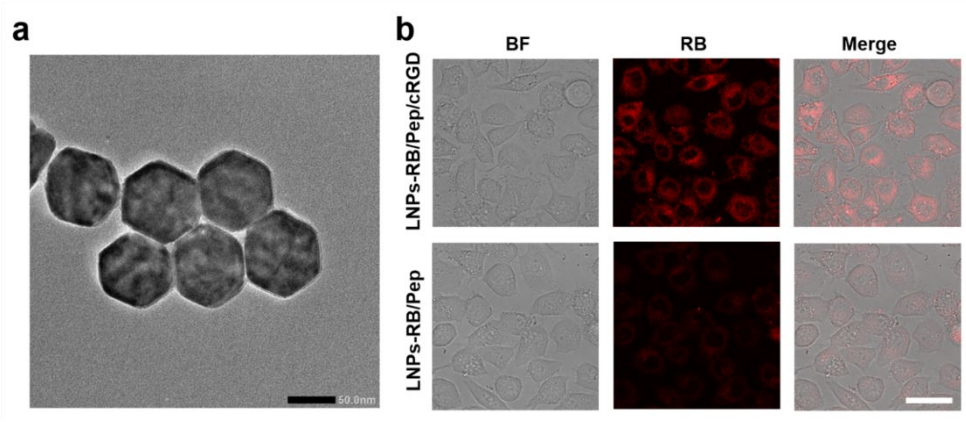

Figure S13. (a) TEM Image of LNPs-RB/Pep/cRGD. Scale bar: 50 nm. (b) Confocal microscopic images of HCCLM3 cells incubated with LNPs-RB/Pep/cRGD (200 μg/mL) and LNPs-RB/Pep (200 μg/mL) for 4h respectively. Scale bar: 75 μm.

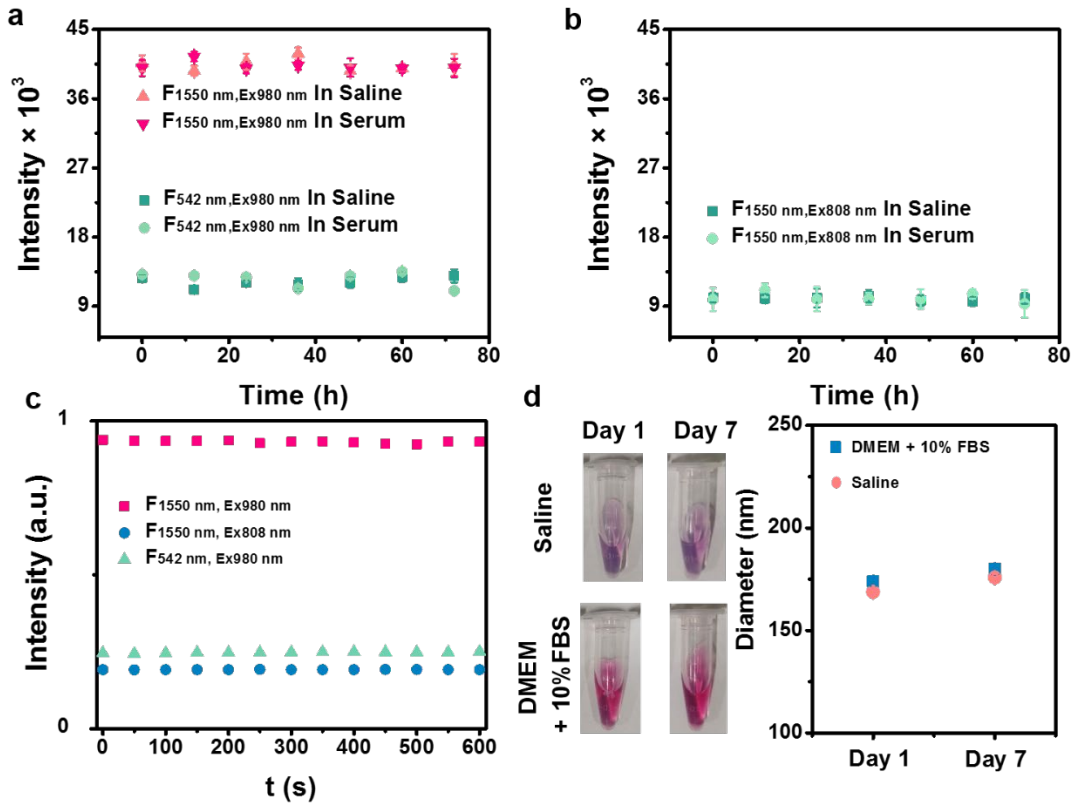

Figure S14. Time dependent luminescence intensity for (a) downconversion emission at 1550 nm and upconversion emission at 542 nm of LNPs-RB/Pep/cRGD (2 mg/mL, 500 μL) in saline/serum under 980 nm excitation and (b) downconversion emission at 1550 nm in saline/serum under 808 nm excitation, (c) Photostability of LNPs-RB/Pep/cRGD under continuous irradiation 10 min with 808 nm (0.05 W/cm^2) and 980 nm (0.05 W/cm^2) lasers. (d) Photos and corresponding DLS values of LNPs-RB/Pep/cRGD incubated in saline and DMEM containing 10% FBS for

7 days. The error bars indicate mean ± S.D. (n = 3).

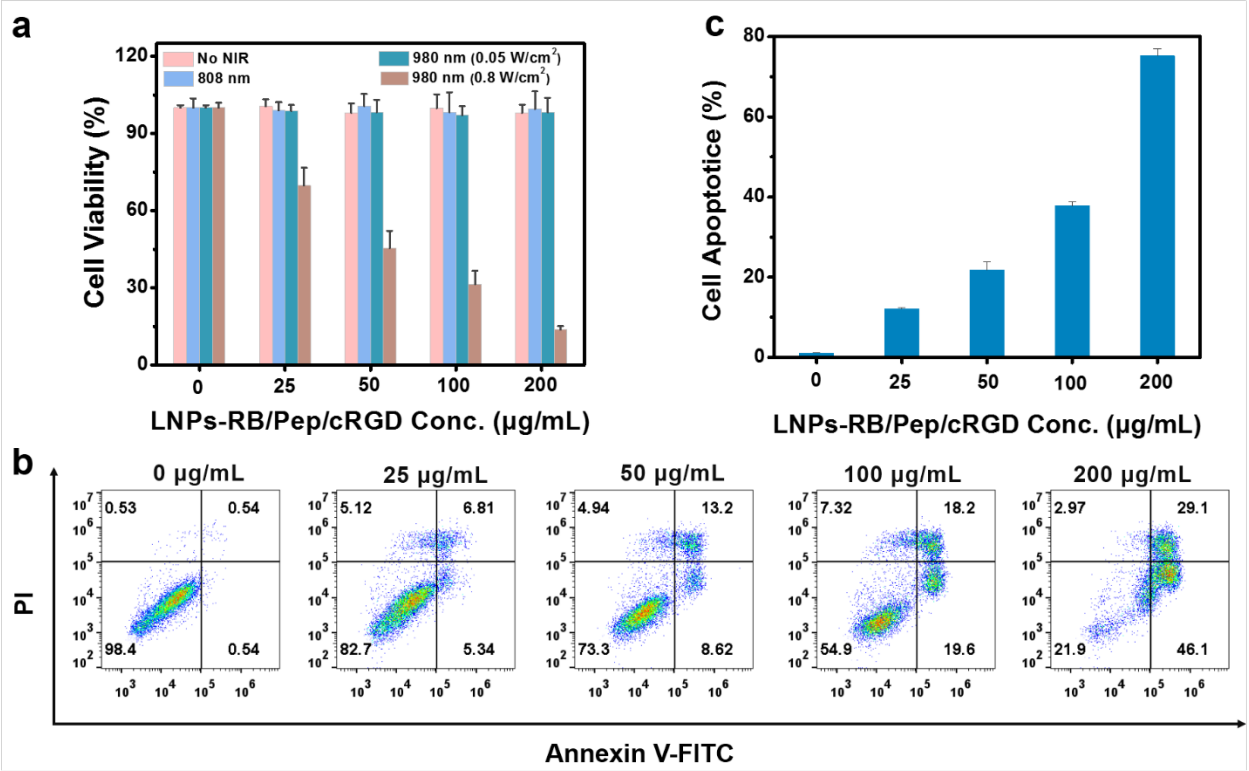

Figure S15. (a) Cell viability of unpretreated HCCLM3 cells (0 μg/mL) and LNPs-RB/Pep/cRGD (25-200 μg/mL) incubated with HCCLM3 cells for 4 h under different condictions of no NIR irradiation, 808 nm NIR irradiation, low power 980 nm NIR irradiation (0.05 W/cm^2), high power 980 nm NIR irradiation (0.8 W/cm^2). (b) Flow cytometry analysis and (c) corresponding cell apoptosis of unpretreated HCCLM3 cells (0 μg/mL) and LNPs-RB/Pep/cRGD (25-200 μg/mL) treated HCCLM3 cells under high power 980 nm NIR irradiation (0.8 W/cm^2). The error bars in a) and c) indicate means ± S.D. (n = 3).

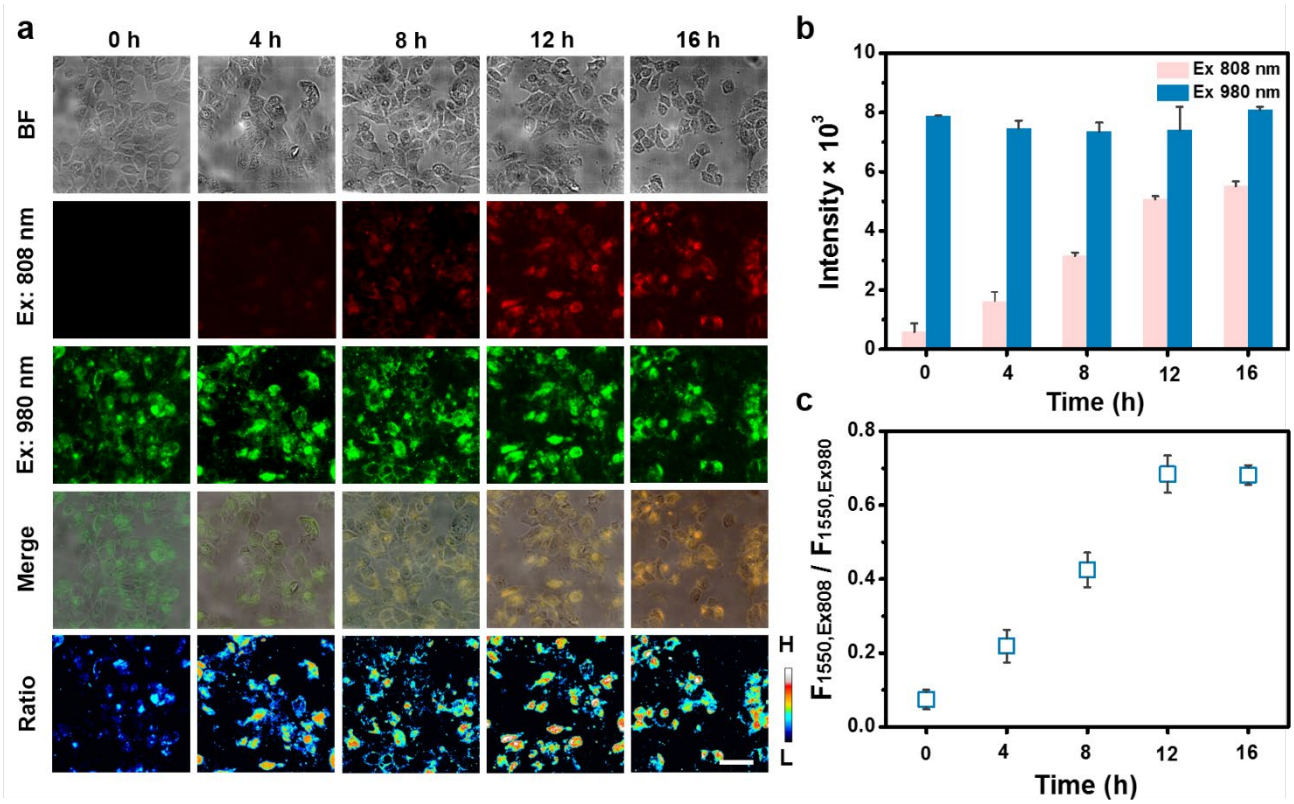

Figure S16. (a) Representative time dependent NIR-IIb fluorescence and ratio images of LNPs-RB/Pep/cRGD treated HCCLM3 cells for 4 h under 808 nm irradiation and low power 980 nm irradiation (0.05 W/cm^2). PDT was performed with 40 min high power 980 nm irradiation (0.8 W/cm^2), and images were taken at different times post PDT (4-16 hours). Scale bar: 100 μm, (b) its corresponding luminescence intensity collected in 1450-1700 nm region under 808 nm irradiation and low power 980 nm irradiation (0.05 W/cm^2) and (c) ratiometric NIR-IIb fluorescence values $F_{1550, Ex808}$ / $F_{1550, Ex980}$. The error bars in b) and c) indicate means ± S.D. (n = 3).

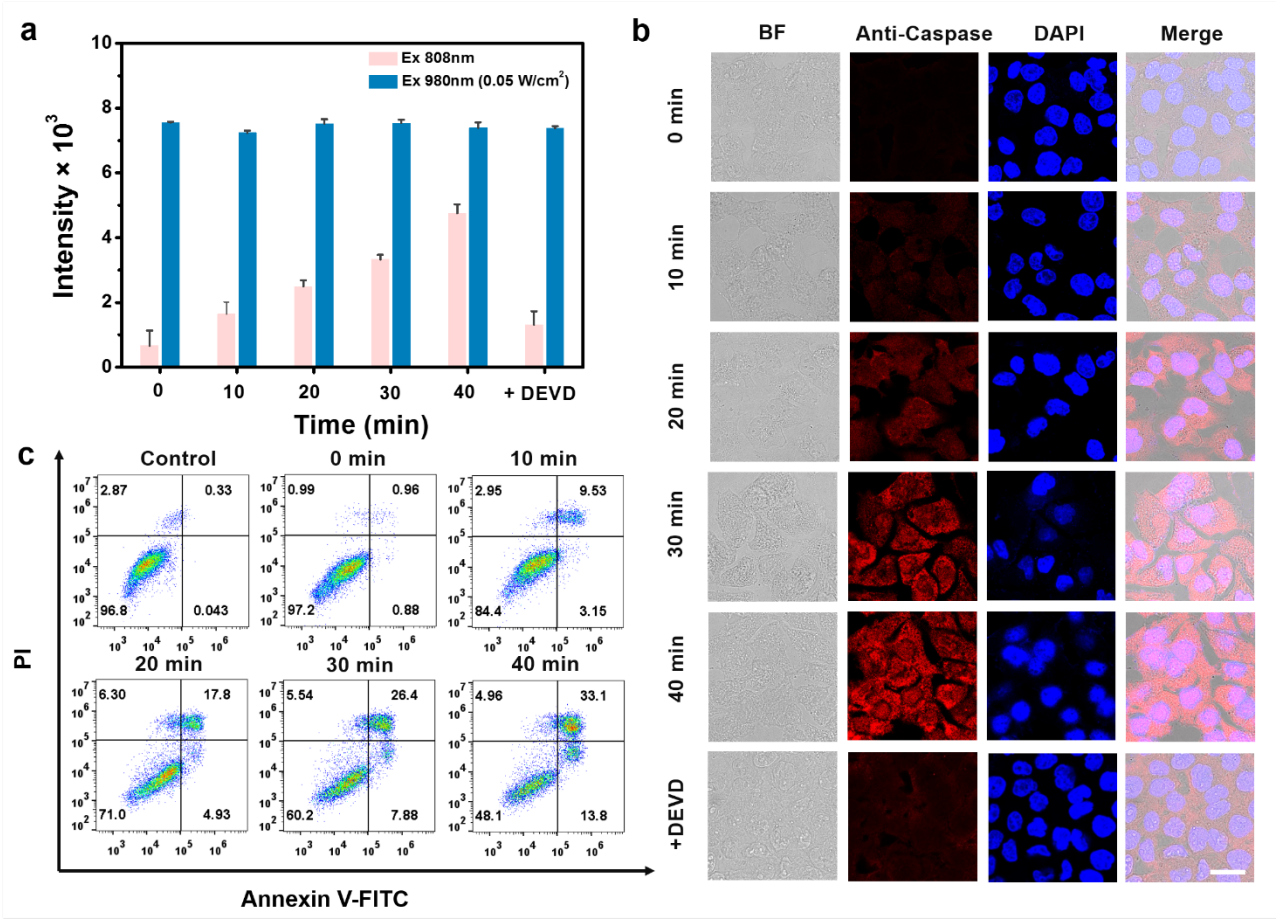

Figure S17. (a) NIR-IIb luminescence intensity for LNPs-RB/Pep/cRGD pretreated HCCLM3 cells under 808 nm and low power 980 nm irradiation (0.05 W/cm^2). (b) Immunofluorescent images of caspase-3 expression for LNPs-RB/Pep/cRGD pretreated HCCLM3 cells for 4 h. Scale bar: 25 μm. PDT was performed with different duration times (0-40 min), Control group (+DEVD) was set by treating HCCLM3 cells with external substrate peptide (CADEVDAK) before PDT. (c) Flow cytometry of HCCLM3 cell (control), LNPs-RB/Pep/cRGD pretreated HCCLM3 cells (0 min), and LNPs-RB/Pep/cRGD pretreated HCCLM3 cells 4 h in response to different PDT periods of 10-40 min. The error bars in a) indicate means ± S.D. (n = 3).

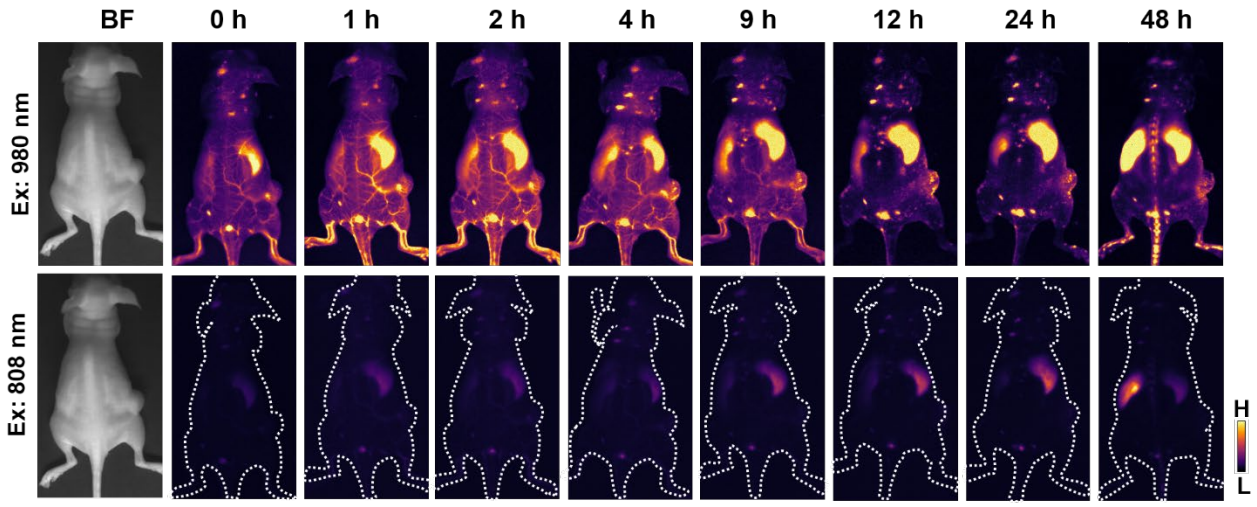

Figure S18. (a) Timespan of NIR-IIb fluorescence imaging in HCCLM3 tumor bearing mice after injection of LNPs-RB/Pep/cRGD under low power 980 nm (0.05 W/cm^2) and 808 nm excitations with LP1500 long-pass filter.

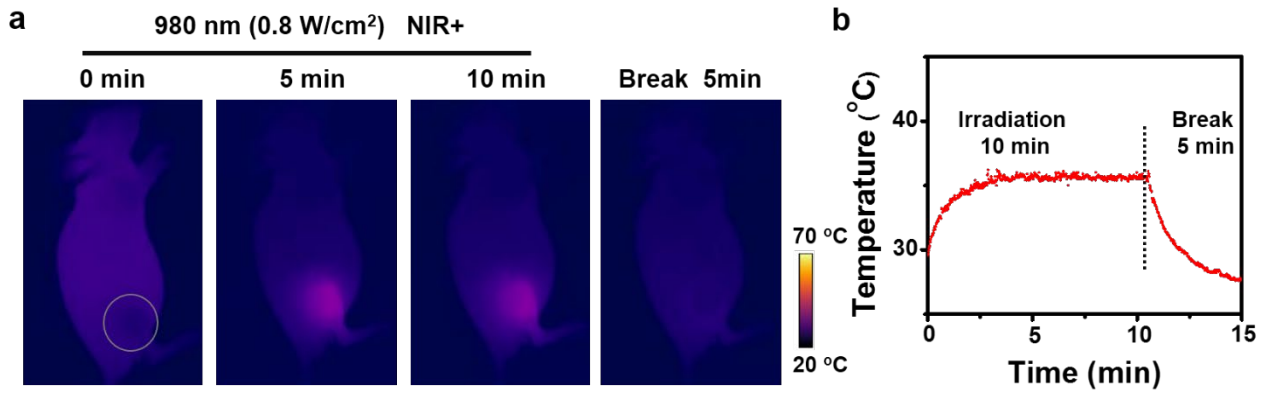

Figure S19. (a) The thermal images of tumor-bearing mice under 980 nm laser excitation at high power (0.8 W/cm^2) for 0 min, 5 min, 10 min, and 5 min "break" period after 10 min exposure, and (b) corresponding temperature change as a function of time.

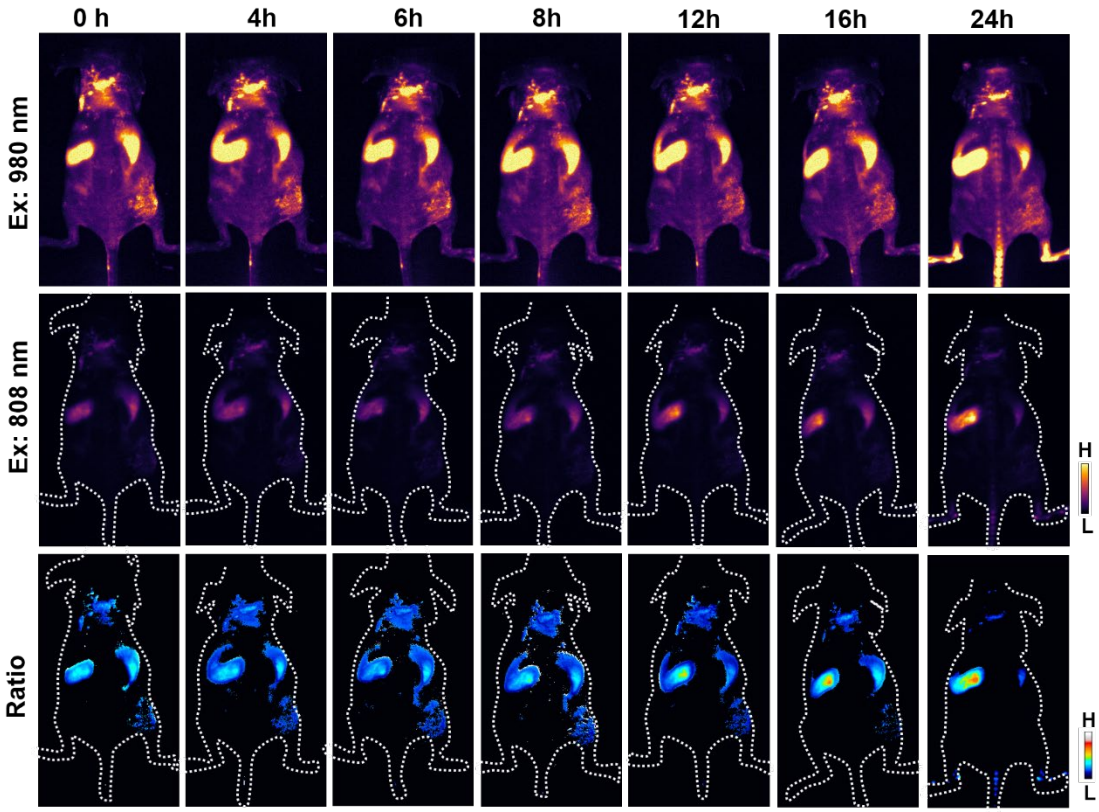

Figure S20. *In vivo* NIR-IIb fluorescence imaging of LNPs-RB/Pep/cRGD injected HCCLM3 tumor bearing mice under low power 980 (0.05 W/cm^2) and 808 nm excitations with LP1500 long-pass filter and corresponding ratio images in the absence of PDT. The image was taken at the same time points as PDT evaluation group.

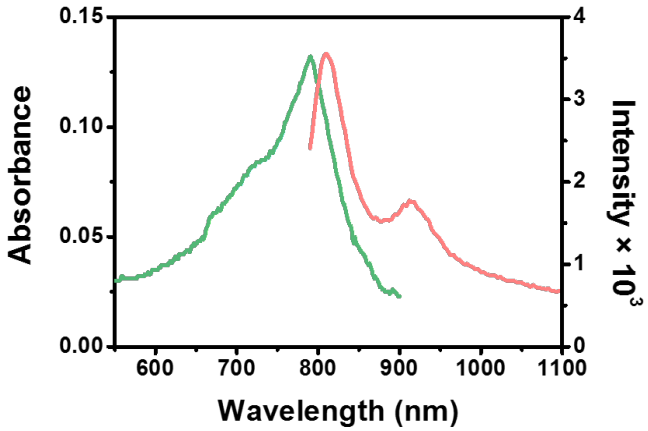

Figure S21. Absorption and fluorescence emission spectra of mice urine collection over 12 h post-PDT.

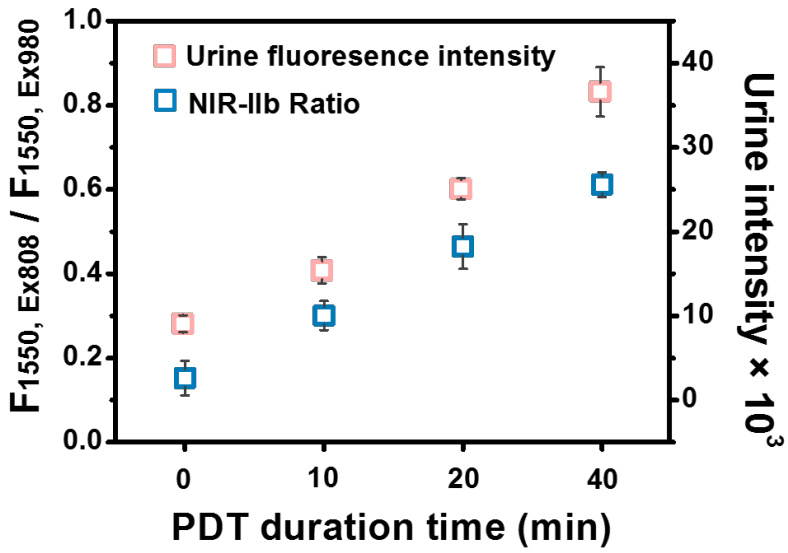

Figure S22. Ratiometric NIR-IIb fluorescence valueand urine fluorescence intensity corresponding to different PDT duration periods. Error bars indicate means ± SD (n = 3).

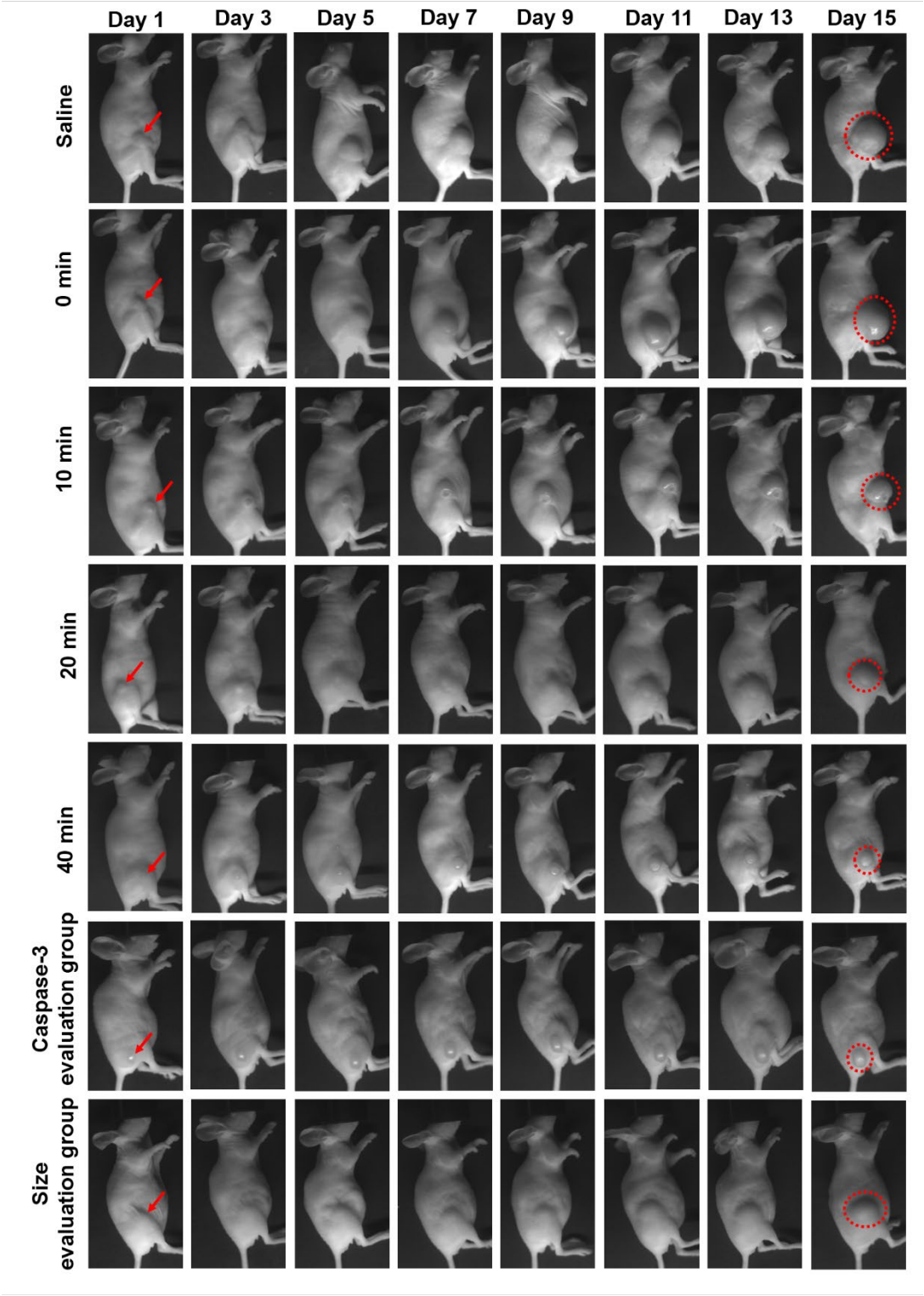

Figure S23. Photographs of mice group treated with saline, LNPs-RB/Pep/cRGD with different duration of PDT periods (0 min, 10 min, 20 min, 40 min) and customized therapeutic group with caspase-3 evaluation and tumor size measurement evaluation respectively. PDT was performed with 5 min break after each 10 min exposure.

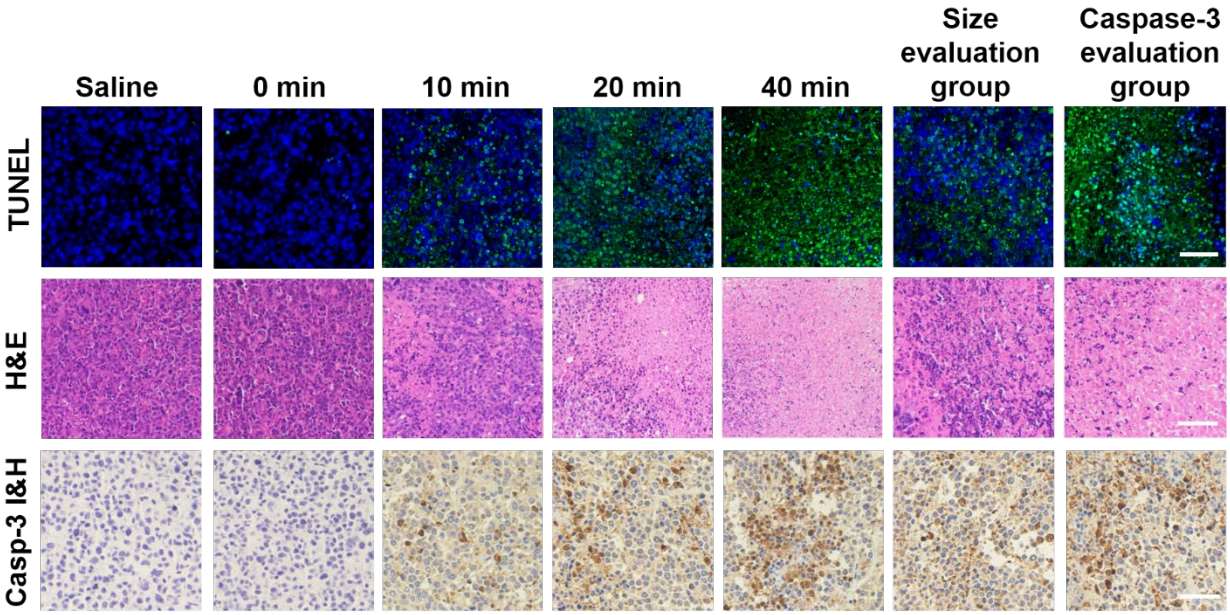

Figure S24. Histological observations of tumor tissues stained with H&E, TUNEL and Casp-3 immunohistochemistry for tumor bearing mice injected with saline, LNPs-RB/Pep/cRGD with different duration of PDT periods (0 min, 10 min, 20 min, 40 min), customized therapeutic group with caspase-3 evaluation and tumor size measurement evaluation, respectively. Scale bar: 50 μm. PDT was performed with 5 min break after each 10 min exposure.

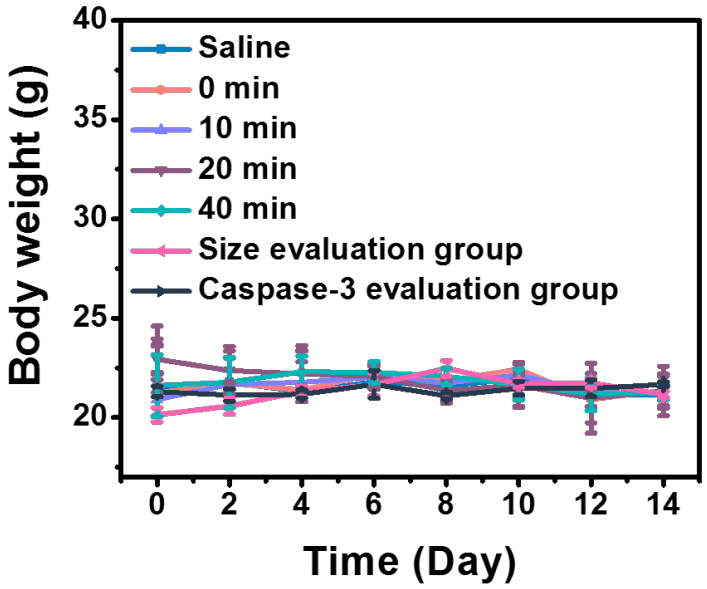

Figure S25. Body weight of tumor bearing mice injected with saline, LNPs-RB/Pep/cRGD with different duration of PDT periods (0 min, 10 min, 20 min, 40 min) and customized therapeutic group with caspase-3 evaluation and tumor size measurement evaluation respectively. Error bars indicate means ± SD (n = 3). PDT was performed with 5 min

break after each 10 min exposure.

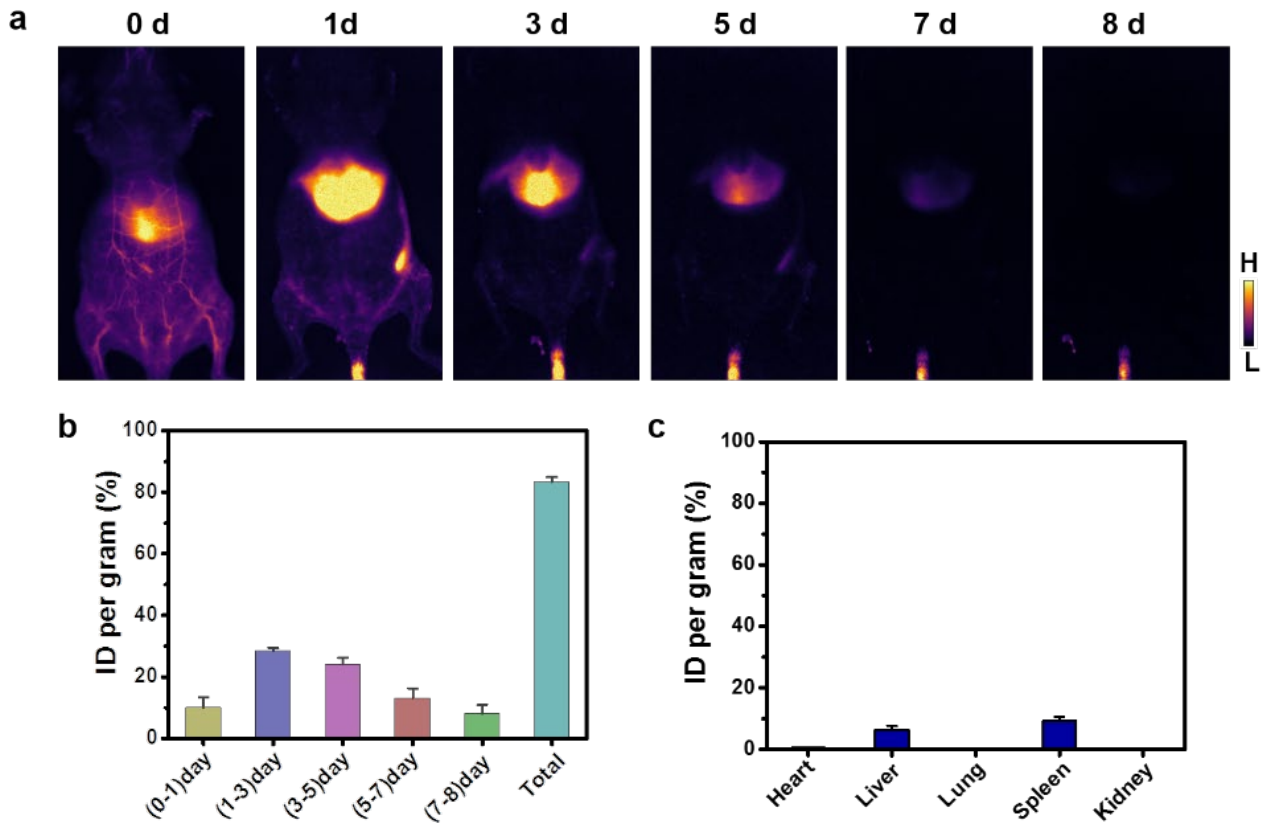

Figure S26. (a) Timespan of *in vivo* NIR-IIb imaging for healthy nude mice after intravenous injection of LNPs-RB/Pep/cRGD under low power 980 nm excitation (0.05 W/cm^2). (b) Percentage of LNPs-RB/Pep/cRGD excreted in feces upto to 8 days after injection (c) Bio-distribution of LNPs-RB/Pep/cRGD in main organs at 8th day post injection obtained by ICP-AES (determination of Gd(III)). The error bars indicate means ± S.D. (n = 3). ID is the abbreviation of injection dose.

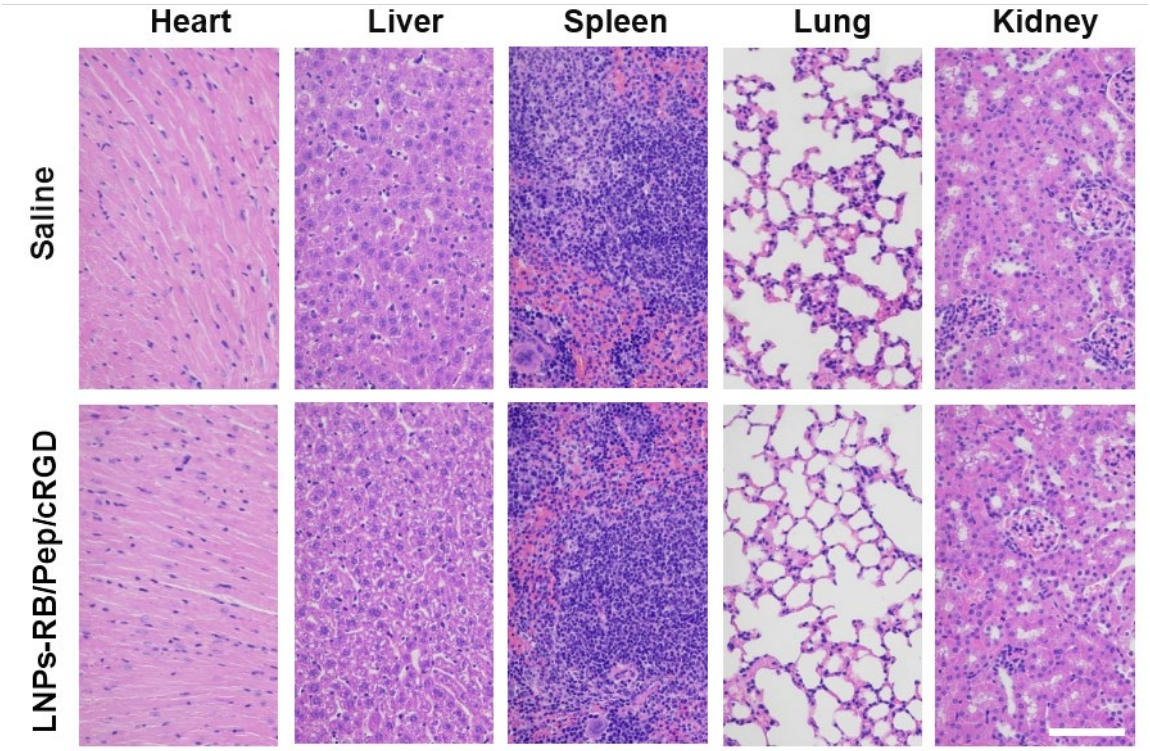

Figure S27. H&E stained histological sections of the organs (heart, liver, spleen, lung, kidney) from saline treated and LNPs-RB/Pep/cRGD treated healthy mice group at 8th day post-injection. Scale bar: 100 μm.

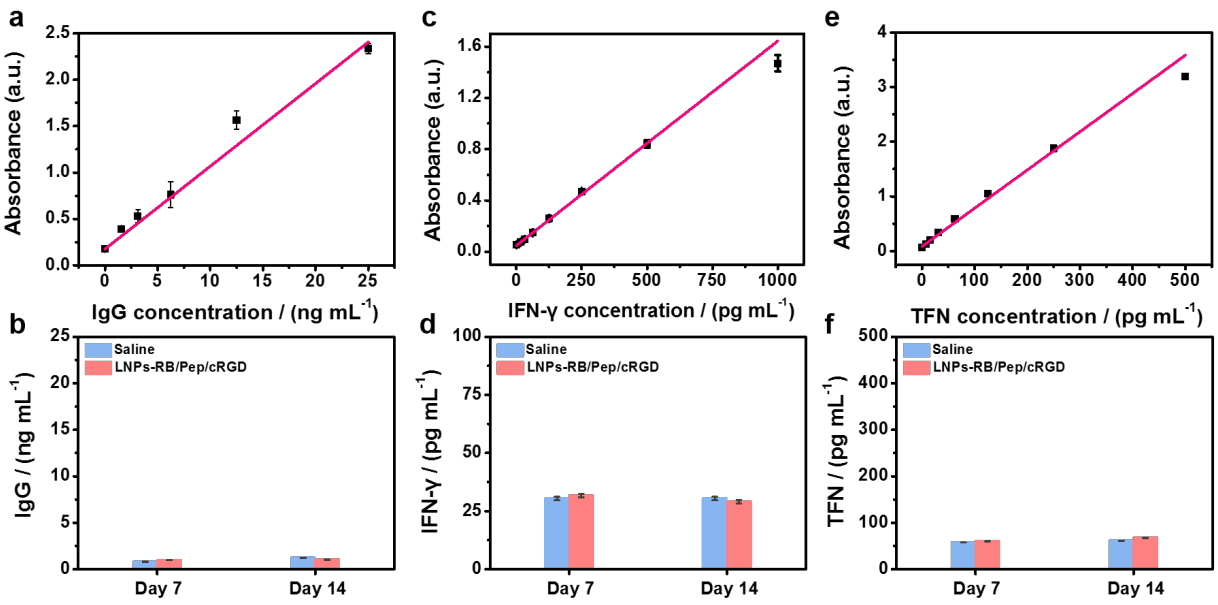

Figure S28. (a) Calibration curves for (a) IgG, (c) IFN-γ and (e) TNF-α detections via ELISA kit and corresponding quantifications of (b) IgG, (d) IFN-γ and (f) TNF-α expressions from saline administrated mice and LNPs-RB/Pep/cRGD (2 mg/mL) administrated mice on days 7 and 14. Error bars indicated means ± SD (n=3).

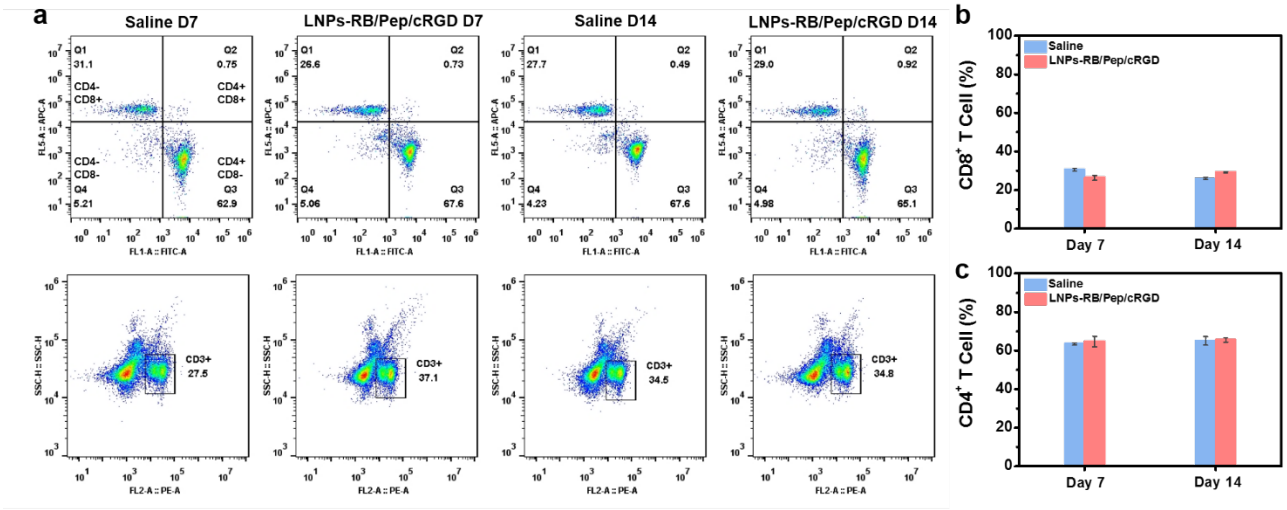

Figure S29. (a) Flow cytometry results and corresponding abundance of (b) CD8+ and (c) CD4+ T cells for mice administrated with LNPs-RB/Pep/cRGD (2 mg/mL) and saline on days 7 and 14. Error bars indicated means ± SD (n=3).

Table 1. List of excitation wavelength and power density for the corresponding figures

Experiment content	NIR irradiation (Power)	Figure number
Up-and downconversion spectrum detection	808 nm/980 nm 1 W/cm^2	Fig. 1c, d, g Supplementary Fig. 2, 7b, c, 9, 10, 12, 14a, b
Photostability detection	808 nm/980 nm 0.05 W/cm^2	Supplementary Fig. 14c
PDT	980 nm 0.8 W/cm^2	Fig. 1f, 2a, b, 3c, 4b, d, h, Supplementary Fig.8, 15, 16a, 17 b, c, 19, 23-25
NIR-II imaging	808 nm/980 nm 0.05 W/cm^2	Fig. 2b, Fig 3c, f, g, Fig. 4b, c, h, i Supplementary Fig. 16a, 18, 20, 26
Thermal images	980 nm 0.8 W/cm^2	Supplementary Fig. 19
Quantum yield detection	808 nm/980 nm 3 W/cm^2	Supplementary Fig. 4

3. References

1 X. B. Zhang, W. W. Chen, X. Y. Xie, Y. Y. Li, D. S. Chen, Z. C. Chao, C. H. Liu, H. B. Ma, Y. Liu and H. X. Ju, *Angew. Chem. Int. Ed.*, 2019, **58**, 12117-12122.

2 X. M. Li, D. K. Shen, J. P. Yang, C. Yao, R. C. Che, F. Zhang and D. Y. Zhao, *Chem. Mater*, 2013, **25**, 106-112.

3 Y. Zhong, Z. Ma, F. Wang, X. Wang, Y. Yang, Y. Liu, X. Zhao, J. Li, H. Du, M. Zhang, Q. Cui, S. Zhu, Q. Sun, H. Wan, Y. Tian, Q. Liu, W. Wang, K. C. Garcia and H. Dai, *Nat. Biotechnol.*, 2019, **37**, 1322-1331.

4 P. Zamani, M. Teymouri, A. R. Nikpoor, J. G. Navashenaq, Z. Gholizadeh, S. A. Darban and M. R. Jaafari, *Eur. J. Cancer*, 2020, **129**, 80-96.